Dielectric mismatch effects in two-electron zero-dimensional nanosystems

J. L. Movilla and J. Planelles*
Departament de Ciències Experimentals, UJI, Box 224, E-12080 Castelló, Spain
(Received 15 June 2006; published 29 September 2006)

Two-electron Coulomb interaction and correlation effects in several spherically symmetric zero-dimensional semiconductor heterostructures are investigated in the large dielectric mismatch regime. Specifically, a semiconductor quantum dot (QD) embedded in air or a vacuum, an air-filled nanocavity in a semiconductor matrix, and a weakly confined D^- center (two electrons bounded to a hydrogenic donor impurity in a QD embedded in air). A strong self-polarization-induced radial localization of the electronic density at the heterojunction interface yields surface states. In these states, the polarization of the electron-electron interaction strongly affects dynamics. For a low dielectric constant of the semiconductor building material, Wigner-like localization of the electronic density occurs. As we increase the dielectric constant, it is gradually suppressed. We prove that this gradual suppression is originated by the enhanced strength of the polarization potential accompanying the increase in permittivity. Additionally, in the presence of a weakly confined D^- center in a QD, a transition phase from volume to surface states takes place. It is characterized, in a wide range of quantum dot radii, by a strong ground state reconstruction and a zero D^- binding energy.

DOI: 10.1103/PhysRevB.74.125322 PACS number(s): 73.21.La, 73.22.−f, 73.20−r, 71.55.−i

I. INTRODUCTION

The effects that dielectric confinement produces on the optical and transport properties of semiconductor heterostructures have been the object of a large amount of theoretical and experimental work.[1–11] These effects are specially relevant in semiconductor zero-dimensional heterostructures (quantum dots, QDs),[12] particularly when the surrounding medium is characterized by a low dielectric response, such as organic polymers, air or a vacuum. Therefore, colloidal semiconductor nanocrystals synthesized by so-called wet chemistry are the proper candidates to undergo the largest dielectric effects, as they usually have small sizes (from 1 to several tens of nanometers) and can be easily isolated and redispersed in the desired medium.[13–18]

Among the theoretical approaches describing the electronic structure of QDs, methods based on the so-called envelope function approximation [or effective mass approach (EMA)] are the most commonly employed.[19,20] Within this approximation the wave-function is factorized as a product of cell-periodic and smooth envelope functions. Next, details of the unit cell are integrated, yielding differential equations for the envelope functions. They are mathematically identical to the Schrödinger equation, but with all microscopic details of the unit cell averaged in their parameters, such as the electron effective mass for electrons and the Luttinger parameter for holes. Indeed, EMA has proved to yield reliable results even in multishell QDs with layers as thin as a single monolayer.[21,22]

The macroscopiclike description of EMA implicitly assumes the screening of carriers by the macroscopic dielectric constant of the medium where they are located. Therefore, if carriers are confined in a QD embedded in a dielectrically mismatched matrix, according to the electrodynamics of continuous media, surface polarization-induced image charges of any excess carriers in the dot should appear.[23] The influence of these image charges on the electronic structure of homogeneous spherical quantum dots is described in the pioneering papers by Brus.[2,24] Thus, two new contributions to the energy of confined carriers arise as the consequence of the dielectric mismatch. On the one hand, there is a single-particle contribution coming from the interaction of carriers with their own induced charges (self-polarization energy), and, on the other hand, there are two-particle contributions coming from the interaction of a carrier with the charge induced by the other one (polarization of the Coulomb interaction).

By assuming infinitely high confinement barriers and steplike dielectric functions, it was proved that dielectric mismatch corrections on excitonic energies in spherical QDs almost totally cancelled each other out,[2,25,26] Coulombic effects being reduced to simple bare electron-hole attraction. The problem of finite barriers and a steplike profile for the dielectric function is quite a lot more involved. This is due to the fact that the self-energy of the partially confined particle diverges, yielding a non-integrable Schrödinger equation. Several solutions have been proposed to overcome this pathology, such as the regularization method,[1,27] or the replacement of the steplike dielectric function by a continuous variation of the dielectric constant within a thin layer of the order of a lattice constant, located at the interface.[6,7] This continuous model for the dielectric function can be justified as follows. On the one hand, the interface between two semiconductors (or between semiconductor and vacuum) is never perfectly sharp, as the steplike model of the dielectric interface assumes. On the other hand, EMA integrates the microscopic details of the unit cell. Therefore, the assumption of a continuous variation of the dielectric constant within a lattice constant-width shell at the interface is also reasonable. These models yield an integrable self-polarization potential. Its profile reveals a slight destabilization in the medium with a higher dielectric constant, and a deep, narrow attractive well in the other medium, close to the interface.[6]

Finite confinement barriers in the presence of dielectric mismatch show qualitative differences with the infinite barrier case. Thus, Bolcatto and Proetto[6] showed that the dielectric effects on exciton energies no longer cancel each other

out. It was also shown that, under specific conditions, the attractive self-polarization potential well is able to confine carriers in surface states, these surface states could even been located on the barrier side of the interface.[27–29] On their hand, Orlandi *et al.*[28] pointed out that these surface states may yield many-body ground state reconstructions that could be monitored, in turn, by transport experiments.

The formation of surface states is more likely when one of the media involved is air or a vacuum [because the depth of the attractive self-polarization potential well of a spherical QD in a given medium is related to $(1/\varepsilon_{>}-1/\varepsilon_{<})/R$, $\varepsilon_{>}$ and $\varepsilon_{<}$ being, respectively, the higher and the lower dielectric constants of the media involved, and R the QD radius]. It should be mentioned that we recently found that the self-polarization well can induce electron trapping in air-filled nanocavities of semiconductor matrices, despite the barrier-acting nature of air.[30] Within these surface states the carriers undergo a strong radial localization, yielding a particular scenario in which inter-particle Coulomb interactions can have important effects on the system dynamics, as we showed in another recent paper,[29] where the influence of image charges on the electron correlation in two-electron spherical QDs was thoroughly investigated. It is shown there that we may face two different limit situations of large dielectric mismatch inducing localization of both electrons in a thin spherical crown at the QD border. Namely, $\varepsilon_{\mathrm{QD}}<\varepsilon_{\mathrm{out}}$ and $\varepsilon_{\mathrm{QD}}>\varepsilon_{\mathrm{out}}$. In either case, the spherical crown is located inside/outside the QD, respectively. When electrons are located inside they behave almost as independent particles while outside they strongly correlate. As the degree of confinement is similar in both cases and the inner/outer effective masses employed in the studied systems are of the same order, the kinetic energy should also be similar. Hence, it is concluded that, while in the first case the electron-electron interaction is negligible in comparison to the kinetic energy, in the second case the opposite should hold.[29] As the electron-electron interaction includes both bare Coulomb plus polarization terms, what must happen is that polarization worked against bare Coulomb in the case of electrons inside while enforced it in the outside case, as can be qualitatively understood from an elementary electrostatic analysis.[35]

In this paper we will show that if the QD is highly insulating (e.g., $\varepsilon_{\mathrm{QD}}<4$ for a 5.35 nm QD radius confined by a 0.9 eV confining barrier height), no surface states can be achieved when this QD is embedded in air or a vacuum, accordingly to previously reported results.[28,29] On bypassing this dielectric constant threshold, a sudden increase in the angular correlation occurs (as the electrons, confined in a narrow crown at the external side of the QD border, exhibit a strong tendency to avoid each other). It is then found that as $\varepsilon_{\mathrm{QD}}$ keeps growing, a monotonous decrease in the angular correlation occurs. We rationalize this finding by looking at the limit case of a conductor QD ($\varepsilon_{\mathrm{QD}}=\infty$), where the strong surface positive polarization charge induced by one electron close to its location, and the corresponding negative charge that it also induces on the opposite site at the QD surface, work against the charge of this electron (which is pushing the second electron away). As a result, the angular correlation decreases. We will show that similar, but enhanced, behavior is found in a two-electron system in a spherical cavity of a semiconductor matrix. Similarities and differences between the two cases are discussed. Finally, we present a comprehensive study on the influence of image charges on electron correlation and interaction energies of a weakly confined D^{-} center (two electrons bounded to a hydrogenic donor impurity) in a semiconductor QD surrounded by air or a vacuum. We show that the combination of one- and two-particle contributions of the dielectric confinement leads to different situations in each system under study, above all when the electronic density is localized in a surface state.

II. THEORETICAL OUTLINE

We will focus our study on the ground state (^1S_g) energies and wave functions of spherical nanostructures containing two interacting conduction band electrons. We employ EMA and a macroscopiclike description of the screening of carriers. Thus, a parameter, the dielectric constant, characterizes the dielectric response of each medium that is involved. The reliability of this approach has been well established for zero-dimensional heterostructures similar to those presented here.[25,31]

The Hamiltonian for two interacting conduction band electrons reads, in atomic units (a.u.),

$$\mathcal{H}(\mathbf{r}_1,\mathbf{r}_2)=\sum_{j=1,2}H_j(\mathbf{r}_j)+V_c(\mathbf{r}_1,\mathbf{r}_2). \tag{1}$$

$V_c(\mathbf{r}_1,\mathbf{r}_2)$ stands for the generalized Coulomb electron-electron interaction, including dielectric mismatch effects. This term can be obtained by solving the Poisson equation, which presents an analytical solution for spherically symmetric QDs when a $\varepsilon(\mathbf{r})=\varepsilon(r)$ steplike dielectric function is assumed. The explicit expressions for $V_c(\mathbf{r}_1,\mathbf{r}_2)$ are given in Ref. 6. $H_j(\mathbf{r}_j)$ represents the one-particle conduction band Hamiltonian of the system

$$H_j(\mathbf{r}_j)=-\frac{1}{2}\boldsymbol{\nabla}\left(\frac{1}{m^*(r_j)}\boldsymbol{\nabla}\right)+V(r_j)+V_s(r_j)+ZV_I(r_j). \tag{2}$$

The first term on the right-hand side of Eq. (2) represents the variable mass hermitic kinetic energy operator.[32,33] A steplike function is employed for the effective mass in order to account for different masses in different materials (m_i^* and m_0^* for the confined and the surrounding medium, respectively). $V(r_j)$ is a steplike function representing the finite spatial confining potential due to the band offset between the media involved. Since, in all the cases studied, the media are air (or a vacuum) and a semiconductor, the depth of the confining well (V_0) is given by the semiconductor electroaffinity. The origin of energies has been set at the bottom of the semiconductor conduction band. $V_s(r_j)$ stands for the self-polarization potential induced by the dielectric mismatch, which can be obtained from $V_c(\mathbf{r}_1,\mathbf{r}_2)$ as

$$V_s(r_j)=\frac{1}{2}V_c(\mathbf{r}_j,\mathbf{r}_j), \tag{3}$$

after excluding the bare Coulomb terms. A smooth variation

of the dielectric constant at the interface has been employed in order to bypass the non-integrability of Eq. (2) when a steplike dielectric function and a finite confinement barrier occur simultaneously. A cosine-like profile within a layer at the interface with a width of 0.3 nm (the order of a lattice constant) is assumed. We have found that, as in Ref. 6, self-energy effects are nearly no sensitive to the smoothing model and to small changes in the interface width.

Finally, $V_I(r_j)$ is the Coulomb potential (including polarization) generated by a shallow donor impurity located at the origin

$$V_I(r_j) = \begin{cases} -\dfrac{1}{\varepsilon_i r_j} - \left(\dfrac{1}{\varepsilon_0} - \dfrac{1}{\varepsilon_i}\right)\dfrac{1}{R} & \text{if } r < R, \\ -\dfrac{1}{\varepsilon_0 r_j} & \text{if } r \geqslant R, \end{cases} \tag{4}$$

where R stands for the interface radius, and ε_i and ε_0 are the dielectric constants of the confined and surrounding media, respectively. Z in Eq. (2) is 1 (0) when the impurity is included (excluded).

The spherical symmetry of the problem allows the angular coordinates of the electron to be integrated analytically in Eq. (2). The radial parts of the exact one-particle wave functions $\phi_{nlm}(\mathbf{r})$ and the corresponding energies are obtained by means of numerical integration (finite differences in a grid extended far beyond the interface radius R). The numerical nature of this integration requires the discretization of the continuous $\varepsilon(r)$ function yielding a multistep profile within the interfacial layer, so that new, artificially introduced divergences are encountered. Such numerical divergences have been overcome by means of a discretization scheme that avoids calculating at the interfaces.[34]

Products of the basis functions ϕ_{nlm} are then used to construct configuration-interaction (CI) expansions $\Psi_{LS}=\Sigma_j \Phi_j$ of the symmetry- and spin-adapted two-electron configurations, where L and S are the total angular and total spin quantum numbers, respectively. The two-electron Hamiltonian containing Coulomb interaction and polarization terms (1) is then diagonalized in the CI basis set. As a result, we get two-particle wave functions $\Psi_{LS}(\mathbf{r}_1,\mathbf{r}_2)$ and energies $E(^{2S+1}L)$. We use as many single-particle basis functions ϕ_{nlm} and as long a CI expansion as are needed to achieve convergence and the required accuracy.

Here we will not use the standard quantum-chemical definition of correlation energy and correlation effects (related to differences between CI and Hartree-Fock variational procedures). Electronic correlation is understood in the present paper as the contribution of the excited configurations to the exact ground state (^1S_g) wave function in comparison to the ground configuration $1s^2$. The quantification of this correlation can be expressed, then, as $c_{\text{corr}}=1-(c_{1s^2})^2$, where c_{1s^2} is the coefficient of the $1s^2$ configuration in the CI expansion.

From the wave functions we define the radial pair density $P(r_1,r_2)$,

$$P(r_1,r_2) = 2\int |\Psi(\mathbf{r}_1,\mathbf{r}_2)|^2 r_1^2 r_2^2 \sin\theta_1 \sin\theta_2 d\phi_1 d\phi_2 d\theta_1 d\theta_2, \tag{5}$$

to study radial correlations, and the angular correlation density $Z(\theta)$,

$$Z(\theta) = N_Z |\Psi[(r_{\max},0,0),(r_{\max},\theta,0)]|^2, \tag{6}$$

with $r_{\max}$ corresponding to the coordinates $r_1=r_2$ of the $P(r_1,r_2)$ maximum and N_Z to the appropriate normalization factor, to study angular correlations.

The D^- center will be characterized by its binding energy E_b, which is defined as

$$E_b(D^-) = E_0 + E(D^0) - E(D^-). \tag{7}$$

Here E_0 is the lowest energy of the Hamiltonian Eq. (2) with $Z=0$, i.e., the single-particle ground state energy of the undoped QD, and $E(D^0)$ and $E(D^-)$ are the single- and the two-particle ground state energies of the doped ($Z=1$) QD, respectively.

III. NUMERICAL RESULTS

A. Quantum dot in air or a vacuum

This section is devoted to studying the effects of the polarization of Coulomb interaction on the electronic correlation of a two-electron QD in the large dielectric mismatch regime (i.e., in the presence of a large QD-surrounding dielectric mismatch leading to a transition from volume to surface states). To this end we consider a two-electron QD similar to the one studied in Ref. 29, defined by an $R=5.35$ nm radius, a $V_0=0.9$ eV confining barrier and an $m^*=0.5$ effective mass. This QD is surrounded by air or a vacuum ($\varepsilon_0=m_0^*=1$). The polarization of the Coulomb interaction is varied from zero ($\varepsilon_{\text{QD}}=1$) up to a maximum value (achieved by a conductor QD, $\varepsilon_{\text{QD}}=\infty$). From a numerical point of view, no significant changes occur beyond $\varepsilon_{\text{QD}}=40-80$, and we limit our study up to this range of QD permittivities.

First of all, we should mention that, as expected, an increase in the dielectric mismatch is accompanied by an increase in radial localization. This is basically a single-particle self-polarization effect. In our case, as the QD surroundings consist of air or a vacuum ($\varepsilon_0=1$), the larger the ε_{QD}, the deeper the self-polarization well and, hence, the stronger the electron localization in this well. The transition from volume to surface states takes place, in our case, at $\varepsilon_{\text{QD}}\sim 4$. This transition can be monitored very well by plotting the radial density or the pair radial density $P(r_1,r_2)$ vs ε_{QD}. The corresponding figures, similar to Figs. 1 and 2 in Ref. 29, have been omitted for the sake of conciseness.

From now on, we should keep in mind that in our case (that is, $\varepsilon_{\text{QD}}>\varepsilon_0$), the surface states are localized in a spherical crown beyond the QD border (outside crown), i.e., the electrons are mostly in a vacuum. Therefore, regardless of the QD permittivity, the electron-electron interaction contains an enhanced bare Coulomb term including a null

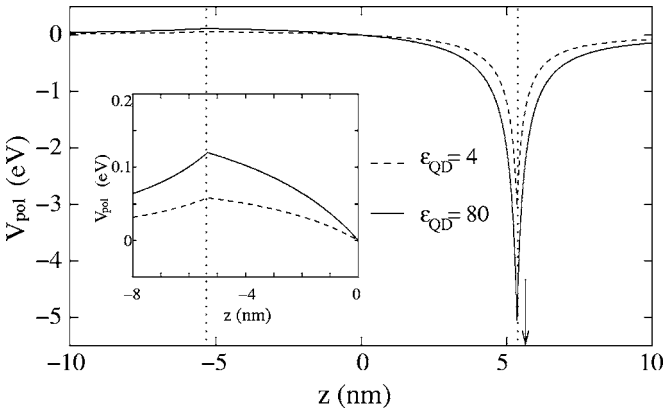

FIG. 1. Coulombic potential V_{pol} generated by the polarization charges induced by an electron located at $(0,0,r_{\max})$, in an outside spherical crown close to the border of a $R=5.35$ nm quantum dot surrounded by air or a vacuum, at the $(0,0,z)$ line. Two different QD dielectric constants are included. Dotted lines indicate the QD edge. The auxiliary arrow indicates the position of the electron producing V_{pol}.

screening ($\varepsilon_0=1$) in the denominator. QD permittivity plays its role in the polarization of the Coulomb interaction (interactions between an electron and the charge induced by the other one).

As the polarization of the dielectric material by a given charge can have a naive view as a set of charges of opposite sign close to its location and of the same sign in the region farthest away from it, we should conclude that polarization works against bare Coulomb, by trying to bring electrons nearer. This naive picture of the Coulomb interaction polarization $V_{\mathrm{pol}}(\mathbf{r}_1,\mathbf{r}_2)$ is quantitatively confirmed in Fig. 1, where a cross section of $V_{\mathrm{pol}}(\mathbf{r}_1,\mathbf{r}_2)$ is represented. In order to draw this figure, the first electron is fixed at $(0,0,r_{\max})$, i.e., at the bottom of the self-polarization well (the maximum of the electron density) along the z axis. The second electron is allowed to move along the line $(0,0,z)$. Two profiles corresponding to $\varepsilon_{\mathrm{QD}}=4$ and 80 are included. We see that this picture is a quantitative counterpart of our simplified reasoning stated above. On the one hand, the higher $\varepsilon_{\mathrm{QD}}$ is, the more relevant V_{pol} turns to be. On the other hand, V_{pol} is strongly attractive near $z=R=5.35$ nm and it is repulsive close to $z=-R=-5.35$ nm, where, according to our naive explanation, we meet opposite and same sign polarized charges, respectively.

An immediate consequence is that angular correlation should decrease as $\varepsilon_{\mathrm{QD}}$ increases, thus pushing the polarization of the Coulomb interaction up. This can be seen in Fig. 2, where $Z(\theta)$ is plotted vs θ for $\varepsilon_{\mathrm{QD}}=4$ and 80, respectively.

In the previous section we defined a numerical parameter $c_{\mathrm{corr}}=1-(c_{1s^2})^2$ to account for electron correlation in a very simple way. We will now use it to gain a deeper understanding of the influence of polarization on the system dynamics. To this end, we plot it in Fig. 3 vs $\varepsilon_{\mathrm{QD}}$ (set of data labeled as $P1$). By looking at this figure we can see that, initially, in the range $1<\varepsilon_{\mathrm{QD}}<3$, c_{corr} exponentially decreases vs $\varepsilon_{\mathrm{QD}}$. We deal with volume states in this range (surface states arise for $\varepsilon_{\mathrm{QD}}=4$ and beyond). If, in a simplified reasoning, we disregard the still small polarization effects, we can rationalize the decrease in correlation as coming from an increase in the screening arising in the dominant bare Coulomb term.[36]

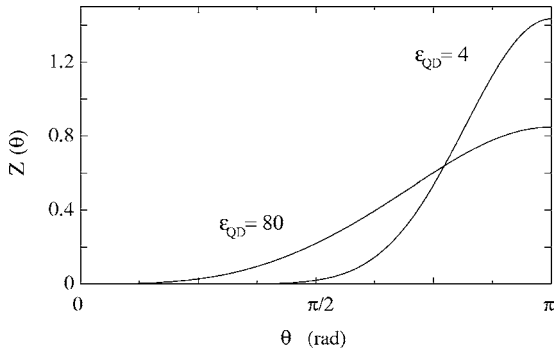

FIG. 2. Angular correlation density $Z(\theta)$ corresponding to a $R=5.35$ nm, $m_i^*=0.5$, $V_0=0.9$ eV quantum dot in air or vacuum, for two different QD dielectric constants.

The following abrupt increase in c_{corr}, shown in Fig. 3, reveals the transition from volume to surface states. These states are localized in an outside spherical crown close to the QD border. Two relevant facts go in parallel to this phase transition. On the one hand, the screening parameter of the bare Coulomb term also undergoes a sudden transition from $\varepsilon_{\mathrm{QD}}$ up to ε_0, with the corresponding sudden increase in the bare electron-electron repulsion, which contributes in turn to an (also abrupt) increase in correlation. On the other hand, the electronic density suddenly moves from the QD center region to the external crown. This transition goes in parallel with a sudden increase in the contribution of $l\neq 0$ orbitals, with a node at the QD center, to the CI wave function. As shown in Ref. 29, only a few configurations have relevant coefficients in the CI expansion of the ${}^1S_g$ surface ground state, the $1p^2$ configuration being, by far, the most relevant one. Our present calculations confirm this fact, and the set of data with the label $|c_{1p^2}|^2$ in Fig. 3 shows the evolution of the contribution of this most relevant excited configuration vs $\varepsilon_{\mathrm{QD}}$. It can be clearly seen how this set of data parallels c_{corr} (labeled as $P1$).

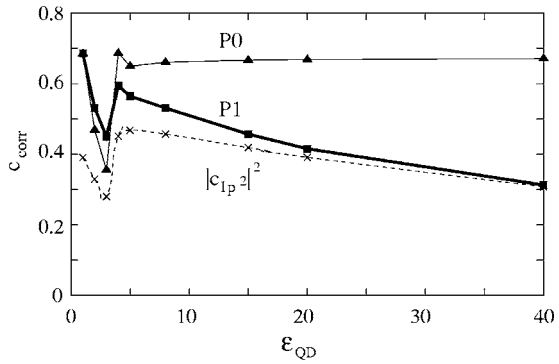

FIG. 3. Two-electron quantum dot in air. $c_{\mathrm{corr}}=1-(c_{1s^2})^2$ and square CI coefficient of the most relevant excited $1p^2$ configuration as a function of the QD dielectric constant $\varepsilon_{\mathrm{QD}}$. $P0$ ($P1$) series represents c_{corr} in the absence (presence) of polarization of the electron-electron interaction. Lines are only guides for the eye.

Once the phase transition has taken place, c_{corr} shows a new gradual decrease vs ε_{QD}. Indeed, the bare Coulomb term cannot contribute to it, as it is approximately constant (since the screening parameter coming into it is ε_0 and not ε_{QD}). Then, the driving force for this new decrease in correlation, as ε_{QD} increases, must be the growing polarization of the Coulomb interaction, which works against the bare Coulomb term. It is confirmed in Fig. 3, where c_{corr} is determined in a set of calculations in which we have artificially removed the polarization of the Coulomb interaction term (set of data labeled as $P0$).[37]

B. Air-filled nanocavities in semiconductor matrices

We have recently reported that self-polarization can induce electron trapping in the air-filled nanocavities of a semiconductor matrix.[30] This trapping occurs in surface states localized in an inside spherical crown close to the cavity border. Therefore, the electron density is mainly located in the barrier-acting air region. In the present paper we report, to our knowledge, the first set of CI calculations of a two-electron system trapped in a spherical nanocavity. As in the previous section, we focus our study on the effects that the polarization of the Coulomb two-body interaction has upon the electron correlation. For a proper comparison with the above presented results, an $R=5.35$ nm air-filled spherical barrier-acting ($V_0=0.9$ eV) nanocavity ($m_C^*=\varepsilon_C=1$) in a semiconductor matrix defined by $m_M^*=0.5$, and several values of $\varepsilon_M \geq 4$ (which ensures electron-trapping in this nanocavity) is considered.

This is a problem similar to that of QD in air. Coming back to the naive description of polarization of the Coulomb interaction, we may say that an electron in the inside crown induces positive charges on the cavity surface, mainly close to its location, and negative charges in the regions farthest away from it, i.e., at infinity or, in other words, no negative charges influencing the second electron are induced. Therefore, a stronger polarization potential with no repulsive character anywhere can be expected. This reasoning is confirmed by calculations. Thus, the same cross section of $V_{pol}(\mathbf{r}_1,\mathbf{r}_2)$ as in Fig. 1, but for the two-electron system in a nanocavity is plotted in Fig. 4 for the same values of the dielectric semiconductor permittivity, namely, $\varepsilon_M=4$ and 80. Indeed, we can see in Fig. 4 that V_{pol} is always negative (attractive) and, by comparison with Fig. 1, we can also see that it is stronger than the one corresponding to a QD in air. Therefore for electrons in a nanocavity one may expect correlation trends similar to those of electrons in the QD surrounded by air, but enhanced. This behavior can be seen in Fig. 5 (which parallels Fig. 3). Note we have only calculated the region of permittivities $\varepsilon_M \geq 4$, since for $\varepsilon_M < 4$ there are no trapped, i.e., bounded, states.

In the region where comparison can be carried out, we observe the same qualitative trends in QDs and nanocavities. Thus, the full calculation ($P1$) shows a decrease in correlation vs ε_M, and the set of calculations only including bare Coulomb ($P0$) display an almost constant correlation. When only bare Coulomb is included ($P0$), the agreement between cavities and QDs is quantitative. However, when full electron-electron interaction is considered ($P1$), nanocavities show lower correlation than QDs, due to the polarization which, as discussed above, is induced more strongly in cavities than in QDs. Extending this reasoning, we also expect nanocavities to have a smaller angular correlation than QDs (the calculations proving this to be the case have not been included for the sake of conciseness).

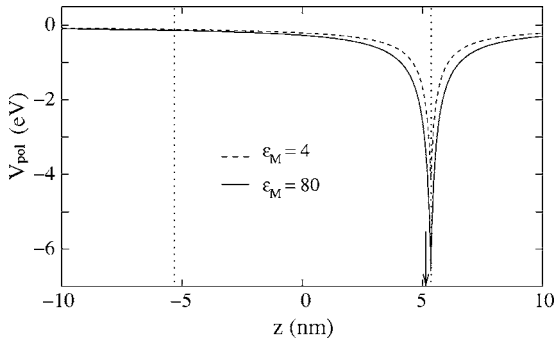

FIG. 4. Coulombic potential V_{pol} generated by the polarization charges induced by an electron located at $(0,0,r_{max})$, in an inside spherical crown close to the border of a $R=5.35$ nm cavity in a semiconductor matrix, at the $(0,0,z)$ line. Calculations for two different matrix dielectric constants are included. Dotted lines indicate the QD edge. The auxiliary arrow indicates the position of the electron producing V_{pol}.

C. Doped quantum dot in air or a vacuum

In this section we investigate the influence of a central shallow donor impurity on the formation of a surface ground state and on the system dynamics of a two-electron QD in air. For the sake of comparison, here we consider the same QD that was defined in Sec. III A but with a hydrogenic impurity located at its center.

As in previous sections, we explore the influence of polarization on electron correlation by plotting the parameter c_{corr} vs ε_{QD} (see Fig. 6). Three regions or phases can be distinguished in this figure. We name them according to their

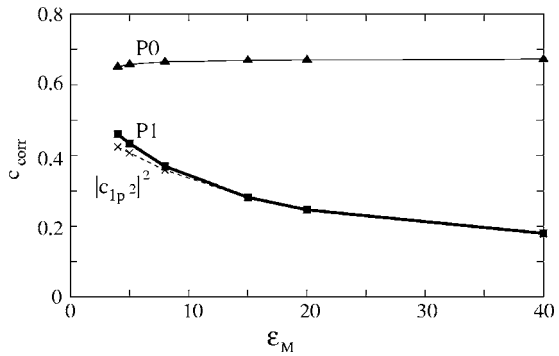

FIG. 5. Two electrons in an air-filled cavity of a semiconductor matrix. $c_{corr}=1-(c_{1s^2})^2$ and square CI coefficient of the most relevant excited $1p^2$ configuration, as a function of the matrix dielectric constant ε_M. $P0$ ($P1$) series represents c_{corr} in the absence (presence) of polarization of the electron-electron interaction. Lines are only guides for the eye.

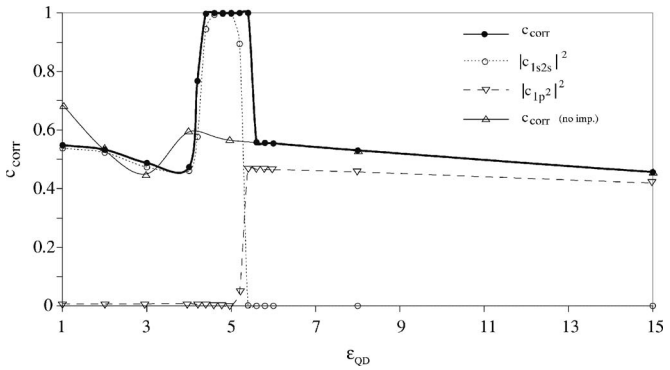

FIG. 6. Two-electrons doped quantum dot in air. $c_{\mathrm{corr}}=1-(c_{1s^2})^2$ and square CI coefficients of the most relevant excited configurations, as a function of the QD dielectric constant $\varepsilon_{\mathrm{QD}}$. Nondoped QD c_{corr} is also enclosed for the sake of comparison. Lines are only guides for the eye.

main physical trend. Namely, impurity ($1<\varepsilon_{\mathrm{QD}}<4.3$), radial-Wigner ($4.3<\varepsilon_{\mathrm{QD}}<5.5$), and angular-Wigner phase ($\varepsilon_{\mathrm{QD}}>5.5$).

In the impurity phase ($1<\varepsilon_{\mathrm{QD}}<4.3$), the confinement regime is weak ($R\ll a_0^*$, a_0^* being the Bohr radius), both electrons are tightly trapped by the impurity potential [see Fig. 7(a), where the radial pair density $P(r_1,r_2)$ for $\varepsilon_{\mathrm{QD}}=4$ is presented[38]] and the system is almost not influenced by the confinement barrier V_0. As for c_{corr}, it decreases vs $\varepsilon_{\mathrm{QD}}$, this trend being related to the growing screening of the electron-electron interaction.

A main difference with the undoped QD is that the most relevant excited configuration coming into the CI expansion of the ${}^1S_g$ ground state is not $1p^2$ but $1s2s$. In this phase, the excited $1s2s$ configuration accounts for most of the correlation in the ${}^1S_g$ ground state.

When $\varepsilon_{\mathrm{QD}}$ goes beyond 4.4, we enter in the radial-Wigner phase. This is revealed in Fig. 6 by an abrupt increase in c_{corr}, which reaches a value close to one, this value being maintained throughout the whole phase. The abrupt c_{corr} change at $\varepsilon_{\mathrm{QD}}=4.4$ is accompanied by a reconstruction of the ${}^1S_g$ ground state, i.e., the dominant configuration of this state undergoes a sudden transition from $1s^2$ up to $1s2s$, thus violating the Aufbau filling rule. The CI $1s2s$ coefficient remains greater than 0.99 throughout all the radial-Wigner phase. This ground state reconstruction involves, in turn, a strong increase in radial correlation, as can be seen in Fig. 7(b), where the radial pair correlation is shown for $\varepsilon_{\mathrm{QD}}=5$. This large radial charge separation can be described as one electron deeply attached to the impurity at the QD center and the other one localized mainly in an outside spherical crown at the self-polarization well. In other words, in this phase, the electronic density experiences a radial-Wigner-like localization.

The last phase transition takes place at $\varepsilon_{\mathrm{QD}}=5.6$ (see Fig. 6), yielding the angular-Wigner phase. Within this phase, the dominant configuration $1s^2$ is recovered and, simultaneously, a fairly relevant contribution of the excited $1p^2$ configuration takes place. These trends are similar to those of the undoped QD, as can be seen in Fig. 6. Indeed, the electronic density distribution shows, as in the case of the undoped QD, a very strong radial localization of both electrons in the self-polarization well [see Fig. 7(c)], and a large angular correlation (not shown for conciseness).

In summary, a two-electron doped QD in air experiences three different phases, depending on the screening capability of its building block material. Low dielectric constants yield the so-called impurity phase, in which impurity is the main driving force for the system dynamics. Intermediate values of $\varepsilon_{\mathrm{QD}}$ monitor the radial-Wigner phase. In this intermediate phase, the impurity still plays a relevant role by trapping one of the electrons close to it. This electron-impurity pair is viewed by the second electron as a neutral-like entity[39] and it therefore behaves as an isolated electron in a QD, choosing the bottom of the self-polarization potential as its favorite location. Finally, large values of $\varepsilon_{\mathrm{QD}}$ are associated with the angular-Wigner phase, where impurity plays a minor role and the two-electron doped QD almost behaves as though it was undoped.

Orbital and binding energies in a doped QD vs $\varepsilon_{\mathrm{QD}}$

This last section is devoted to investigating the influence of the dielectric mismatch on the single-particle energy structure and its relation with the phases encountered in a two-electron doped QD. It is also devoted to studying the evolution of binding energy in the different phases.

Figure 8 represents the energy of the low-lying single-particle orbitals vs $\varepsilon_{\mathrm{QD}}$. In this figure, the range of dielectric

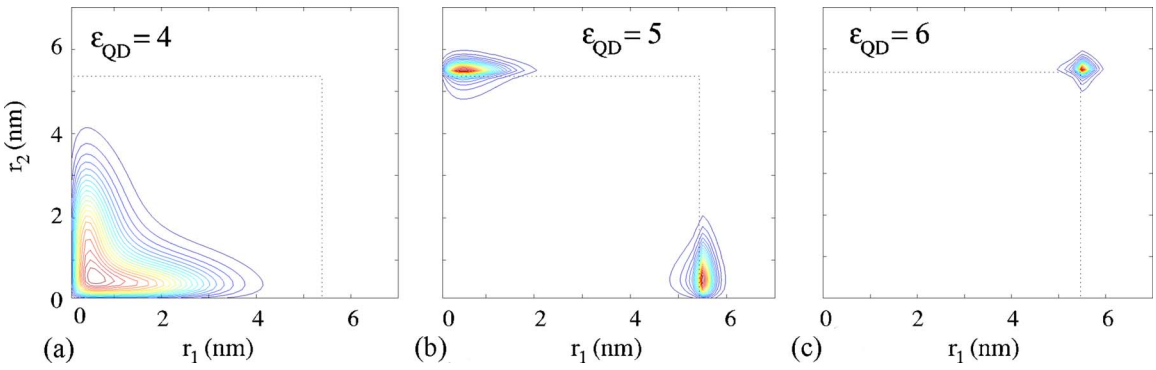

FIG. 7. (Color online) Radial pair densities $P(r_1,r_2)$ of the two-electron ground state of a doped QD in air or a vacuum for three different values of the QD dielectric constant. (a) $\varepsilon_{\mathrm{QD}}=4$, (b) $\varepsilon_{\mathrm{QD}}=5$, (c) $\varepsilon_{\mathrm{QD}}=6$. Dotted lines indicate the quantum dot edge.

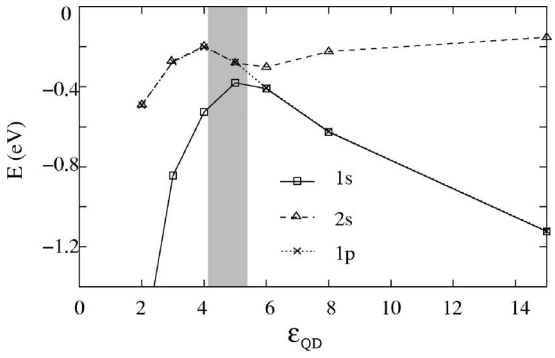

FIG. 8. Energies of the low-lying orbitals $1s$, $2s$, and $1p$, corresponding to a doped QD in air, as a function of its dielectric constant ε_{QD}. In the figure, the range of dielectric constants corresponding to the radial-Wigner phase has been highlighted in order to delimit the range of all three phases occurring in this system. Lines are only guides for the eye.

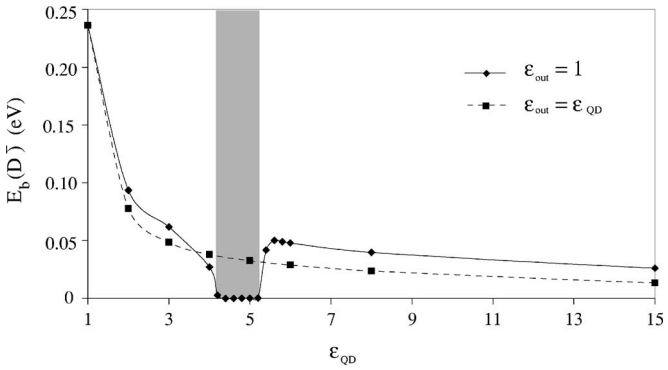

FIG. 9. Binding energy, $E_b(D^-)$ as a function of the doped two-electron QD dielectric constant ε_{QD}. The binding energy resulting when the dielectric effects are disregarded ($\varepsilon_0=\varepsilon_{QD}$) has also been included as a reference. In the figure, the range of dielectric constants corresponding to the radial-Wigner phase has been highlighted in order to delimit the range of all three phases occurring in this system. Lines are only guides for the eye.

constants corresponding to the radial-Wigner phase has been highlighted in order to delimit the range of all three phases. In the low-ε_{QD} region, the low-lying single-particle energy spectrum resembles that of an impurity in an extended medium, i.e., the $1s$ ground orbital is energetically well separated from the nearly degenerated $1p$ and $2s$ orbitals.

As ε_{QD} increases, the self-polarization well becomes deeper and the impurity potential shallower. In the intermediate-ε_{QD} region, orbitals $1p$ and $2s$ are quite stabilized by the self-polarization potential becoming surface states and appearing energetically close to $1s$ (which is still a volume state). An anticrossing between same symmetry orbitals $1s$ and $2s$ then occurs, i.e., the $1s$ orbital concentrates mostly in the self-polarization well while $2s$ turns back into a volume state. Further on, $1s$ and $1p$ become quasidegenerate and increasingly stabilized by the self-polarization well, while $2s$ is left unstabilized.

A key factor for reconstructions and strong correlations is the energy distance between interacting orbitals. Thus, the radial-Wigner phase corresponds to the region where $1s$ and $2s$ are very close. As both orbitals show a very different density distribution (one is close to the QD center while the other is at its surface) Coulomb repulsion is small, so that a reconstruction from $1s^2$ up to $1s2s$ becomes favorable. All the same, the angular-Wigner phase corresponds to the region where $1s$ and $1p$ are quasidegenerate and the formation of an angular-Wigner-like molecule with a minimum Coulomb repulsion arises.

Looking at Fig. 6 one realizes that the radial-Wigner phase occurs in a rather short range of dielectric constants ($4.3<\varepsilon_{QD}<5.5$ for an $R=5.35$ nm QD confined by a barrier of height $V_0=0.9$ eV). On the one hand, we have proved that this phase is robust to large changes in the QD radius. In particular, we fixed $\varepsilon_{QD}=5$ and observed that the radial charge separation remains unaltered for R ranging from 4 to more than 20 nm. On the other hand, we also considered taller confining barriers. In this regard we should remember that the larger the confining barrier is, the larger the value of ε_{QD} required to induce surface states will be. As ε_{QD} rises, the $1p$ orbital stabilizes with respect to the $2s$. If the increase is large, it may give rise to a diffuse phase transition with simultaneous increasing of both radial and angular correlations in a short range of dielectric constants. In other words, the intermediate radial-Wigner phase may eventually be replaced by a diffuse transition from the first to the third phase.

Finally, we calculate the binding energy $E_b(D^-)$ of the doped two-electron QD. The results are summarized in Fig. 9, where the D^- binding energy $E_b(D^-)$ [Eq. (7)] is represented vs the QD dielectric constant. The binding energy in the same case but now disregarding dielectric effects ($\varepsilon_0=\varepsilon_{QD}$) has also been included as a reference. In this last case, $E_b(D^-)$ diminishes monotonically as ε_{QD} increases, due to the enhanced screening of the attractive impurity potential. But when dielectric effects are included, the binding energy is canceled out in the range of existence of the radial-Wigner phase (see Fig. 9). Then, this phase can be considered to be the superposition of one electron in the ground state of a doped QD and the other in the ground state of an independent, undoped QD [see Eq. (7)]. The underlying reason is that the Coulomb potential (including polarization terms) produced by the s-like internal electron is almost totally cancelled out with the one produced by the impurity, thus providing no net effect on the external electron. This external electron then behaves as a single electron in an undoped QD, while the internal electron, located very close to the impurity, is negligibly affected by the electron in the external crown.

IV. CONCLUSIONS

A comprehensive study is carried out to investigate the influence of dielectric mismatch effects on Coulombic correlations and energies in several zero-dimensional two-electron spherical systems, namely, a semiconductor quantum dot in air or a vacuum, an air-filled nanocavity in a semiconductor matrix, and a D^- center confined in a semiconductor quantum dot surrounded by air or a vacuum. We focus our attention on situations in which surface states are formed as a consequence of single-particle self-polarization effects. It is shown that the polarization of the electron-electron interac-

tion induced by the dielectric discontinuity strongly affects interparticle correlations and interaction energies. In addition, the study also demonstrates how the combination of single- and two-particle Coulombic effects may give rise, in weakly confined D^- systems, to the appearance of different phases. Strong, Wigner-like localizations of the electronic density and important reconstructions of the two-electron ground state are found.

The main conclusions of the paper are itemized as follows.

(i) Surface states in QDs surrounded by air or a vacuum may localize the electronic density in the external medium, and, then, electrons undergo a strong angular correlation. This correlation is gradually reduced as the QD dielectric constant increases, due to the influence of the polarization charges induced at the dielectric interface.

(ii) In the case of surface states in air-filled nanocavities of semiconductor matrices, polarization charges reduce the electronic correlation to a greater extent than in the QD case.

(iii) A transition phase from volume to surface states accompanied by a strong radial Wigner-like localization of the electronic density is produced when a quantum dot is doped with a central shallow donor impurity in the weak confinement regime. Within this phase, the D^- center presents zero binding energy, providing a situation in which the system behaves as a twofold electron reservoir. We show that the impurity is able to attach the first excess electron strongly. However, this electron totally blocks the effect of the impurity, and the system now behaves as an undoped (and empty) QD for the second excess electron.

(iv) The radial-Wigner phase vanishes as we approach the strong confinement regime. However, it is stable within a wide range of QD sizes, thus making its experimental search and characterization feasible.

ACKNOWLEDGMENTS

Financial support from MEC-DGI Project No. CTQ2004-02315/BQU and UJI-Bancaixa Project No. P1-B2002-01 (Spain) is gratefully acknowledged. A Spanish MECD FPU grant is also acknowledged (J.L.M.).

*Electronic address: planelle@exp.uji.es

[1] L. Bányai and S. W. Koch, *Semiconductor Quantum Dots* (World Scientific, Singapore, 1993).
[2] L. E. Brus, J. Chem. Phys. **80**, 4403 (1984).
[3] V. A. Fonoberov, E. P. Pokatilov, and A. A. Balandin, Phys. Rev. B **66**, 085310 (2002).
[4] L. Bányai, I. Galbraith, C. Ell, and H. Haug, Phys. Rev. B **36**, 6099 (1987).
[5] T. Takagahara, Phys. Rev. B **47**, 4569 (1993).
[6] P. G. Bolcatto and C. R. Proetto, J. Phys.: Condens. Matter **13**, 319 (2001).
[7] F. Stern, Phys. Rev. B **17**, 5009 (1978).
[8] M. Iwamatsu, M. Fujiwara, N. Happo, and K. Horii, J. Phys.: Condens. Matter **9**, 9881 (1997).
[9] G. Goldoni, F. Rossi, and E. Molinari, Phys. Rev. Lett. **80**, 4995 (1998).
[10] A. Franceschetti, A. Williamson, and A. Zunger, J. Phys. Chem. B **104**, 3398 (2000).
[11] R. Tsu and D. Babić, Appl. Phys. Lett. **64**, 1806 (1994).
[12] Z. Y. Deng, J. K. Guo, and T. R. Lai, J. Phys.: Condens. Matter **6**, 5949 (1994).
[13] A. Mews, A. Eychmüller, M. Giersig, D. Schoos, and H. Weller, J. Chem. Phys. **98**, 934 (1994).
[14] A. P. Alivistatos, Nature (London) **271**, 933 (1996).
[15] A. Mews, A. V. Kadavanich, U. Banin, and A. P. Alivisatos, Phys. Rev. B **53**, R13242 (1996).
[16] R. B. Little, M. A. El-Sayed, G. W. Bryant, and S. Burke, J. Chem. Phys. **114**, 1813 (2001).
[17] D. J. Norris and M. G. Bawendi, Phys. Rev. B **53**, 16338 (1996).
[18] Special Issue on Spectroscopy of Isolated and Assembled Semiconductor Nanocrystals, J. Lumin. **70** (1-6) (1996).
[19] G. Bastard, *Wave Mechanics Applied to Semiconductor Heterostructures* (Les Éditions de Physique, Les Ulis, 1988).
[20] J. P. Loehr, *Physics of Strained Quantum Well Lasers* (Kluwer Academic, Boston, 1998).
[21] G. W. Bryant and W. Jaskólski, Phys. Rev. B **67**, 205320 (2003).
[22] J. J. Shi, Chin. Phys. **11**, 1286 (2002).
[23] J. D. Jackson, *Classical Electrodynamics* (Wiley, New York, 1962).
[24] L. E. Brus, J. Chem. Phys. **79**, 5566 (1983).
[25] M. Lannoo, C. Delerue, and G. Allan, Phys. Rev. Lett. **74**, 3415 (1995).
[26] P. G. Bolcatto and C. R. Proetto, Phys. Rev. B **59**, 12487 (1999).
[27] L. Bányai, P. Gilliot, Y. Z. Hu, and S. W. Koch, Phys. Rev. B **45**, 14136 (1992).
[28] A. Orlandi, G. Goldoni, F. Mangui, and E. Molinari, Semicond. Sci. Technol. **17**, 1302 (2002).
[29] J. L. Movilla, J. Planelles, and W. Jaskólski, Phys. Rev. B **73**, 035305 (2006).
[30] J. Planelles and J. L. Movilla, Phys. Rev. B **73**, 235350 (2006).
[31] L. W. Wang and A. Zunger, Phys. Rev. Lett. **73**, 1039 (1994).
[32] D. BenDaniel and C. B. Duke, Phys. Rev. **152**, 683 (1966).
[33] P. Harrison, *Quantum Wells, Wires and Dots* (Wiley, Chichester, 2001).
[34] J. L. Movilla and J. Planelles, Comput. Phys. Commun. **170**, 144 (2005).
[35] Once a prominent role of the bare Coulomb term between the electrons located in the crown on the vacuum side is assumed, pushing either electron to an opposite site in this outside crown.
[36] In these volume states, carriers are almost completely confined inside the QD border. Then, the dielectric constant coming into the bare Coulomb term is ε_{QD}.
[37] Care should be taken when talking about splitting the electron-electron interaction energy into a sum of bare Coulomb and polarization. Indeed, the so-called bare Coulomb term may include dielectric polarization. For example, the interaction between two electrons in a completely uniform medium (so that no polarization terms coming from dielectric mismatches arise) with permittivity $\varepsilon \neq 1$ is given by the bare Coulomb term $e^2/\varepsilon r$.

It still includes the polarization of the dielectric medium, screening the vacuum bare Coulomb e^2/r term. In this sense, please note that there is no contradiction between the limit values that the bare Coulomb term may reach for very large values of ε_{QD} in the case of a high/low V_0 confining QD barrier, which does not allow/allows the formation of surface states. In the first instance, the bare Coulomb term goes to zero as the dividing screening factor ε_{QD} increases greatly. In the second case, we find a value of $1/R$ a.u. (which corresponds to the work required to bring an electron from infinity up to the border of a radius R QD when a unit charge is uniformly distributed in an outside spherical crown by this border).

[38] Note that the radial pair density $P(r_1,r_2)$, Eq. (5), includes the differential surfaces $dS_i=r_i^2 \sin\theta_i d\theta_i d\phi_i$ in its definition. It is therefore necessarily zero at the origin, $r_1=r_2=0$. However, this does not mean at all that the wave function has a node at the origin.

[39] Within the radial-Wigner phase, the electron-electron Coulomb repulsion is nearly independent of ε_{QD} and can be accurately estimated by $1/\varepsilon_0 r_{max}$. This same value, but with opposite sign, corresponds to the (attractive) interaction of the unit negative charge located in the outside crown and the central hydrogenic impurity. Both interactions lead, then, the second electron to feel nearly free, within the region where it is confined.